RESIDUAL GAS ANALYSIS
OF CERAMIC DIP PACK
SEMICONDUCTOR DEVICES

THESIS

Presented to the Graduate Council of

Southwest Texas State University

in Partial Fulfillment of

the Requirements

For the Degree of

MASTER OF SCIENCE

BY

David L. Meeker; B. S.
(San Marcos, Texas)

August, 1986

ACKNOWLEDGEMENTS

The author would like to express his gratitude to the faculty and staff of the physics department at Southwest Texas State University, all of whom helped me with their encouragement, enthusiasm and guidance. A special thanks goes to Dr. Victor Michalk and Dr. Robert Anderson, for their assistance.

David L. Meeker

August, 1986

San Marcos, Texas

TABLE OF CONTENTS

	Page
LIST OF ILLUSTRATIONS	v
LIST OF TABLES	vi
FOREWORD	1
INTRODUCTION	1
Chapter	
1. THEORETICAL BACKGROUND OF RESIDUAL GAS ANALYSIS	2
2. EXPERIMENTAL METHODS	7
A. Preparation of the Ceramic Package	7
B. Procedure	12
3. INVESTIGATION OF THE DATA	14
A. Analysis	14
B. Ion Analysis	36
C. Conclusions	41
4. SUGGESTIONS FOR FURTHER RESEARCH	42
A. Packagebreaker Additions and Modifications	42
B. System Additions and Modifications	42
C. Preparation of the Ceramic Package	43
D. Data Acqusition	43
REFERENCES	45
BIBLIOGRAPHY	46

LIST OF ILLUSTRATIONS

Page

1. Stable Region of Operation for the QUAD 1210 5
2. Photograph: Exploded View of Packagebreaker 8
3. Photograph: Diffusion Oil Pump System 9
4. Photograph: Breaker-Detector System Segment 10
5. Photograph: Ion Pump and System Controls 11
6. Photograph: Segmented Data Samples from Device 3 15
7. Photograph: Initial Trace before Device 4 Rupture 17
8. Photograph: Immediatly after Device 4 Rupture 17
9. Photograph: .41 Seconds after Device 4 Rupture..... 17
10. Photograph: .82 Seconds after Device 4 Rupture..... 18
11. Photograph: 1.23 Seconds after Device 4 Rupture..... 18
12. Photograph: 1.64 Seconds after Device 4 Rupture..... 18
13. Photograph: 2.05 Seconds after Device 4 Rupture..... 19
14. Photograph: 2.46 Seconds after Device 4 Rupture..... 19
15. Photograph: 2.87 Seconds after Device 4 Rupture..... 19
16. Photograph: 3.28 Seconds after Device 4 Rupture 20
17. Photograph: 3.69 Seconds after Device 4 Rupture..... 20
18. Photograph: 4.10 Seconds after Device 4 Rupture..... 20
19. Photograph: 4.51 Seconds after Device 4 Rupture..... 21

LIST OF TABLES

1. Residual Gases Present in Device 3 16

2. Data Obtained from Analysis of Figure 7 22

3. Data Obtained from Analysis of Figure 8 23

4. Data Obtained from Analysis of Figure 9 24

5. Data Obtained from Analysis of Figure 10 25

6. Data Obtained from Analysis of Figure 11 26

7. Data Obtained from Analysis of Figure 12 27

8. Data Obtained from Analysis of Figure 13 28

9. Data Obtained from Analysis of Figure 14 29

10. Data Obtained from Analysis of Figure 15 30

11. Data Obtained from Analysis of Figure 16 31

12. Data Obtained from Analysis of Figure 17 32

13. Data Obtained from Analysis of Figure 18 33

14. Data Obtained from Analysis of Figure 19 34

15. Typical Mass Patterns for Residual Gas Analyzers 35

16. Solid Materials Deposited and Removed With Gases Used for the Plasma Process 37

17. Chemicals Used in Assembly, Capacitor Construction, and Film Resistor Construction 38

18. Chemicals Used for Etch Preparation, Doping Chemicals, and Etchant Formulas for Alumina Substrates 39

LIST OF TABLES

Page

19. Reactive Ion Etchants of Aluminum Alloys Used in MOS Circuits, Some Weights of Possible Etchant Ions Formed During Ionization 40

FOREWORD

Device failure has become a necessary of the semiconductor industry. A great deal of time and effort is given to finding the reason a device failed. Some of the reasons for failure may be poor contacts, defective masking, impropper cleaning, etc.. In addition to these causes the thin films may absorb acids, gases, etc. which may prove to be corrosive after a time. It is the purpose of this work to find a way to detect these gases and attempt to determine if any might contribute to device failure.

INTRODUCTION

To determine what residual gases are present, if any, the problem of violating a military grade 14 pin ceramic dip package in a hard vacuum must be solved. This was done by the use of two modified vacuum valves, a wedge and a holder. The volume of the interior of an integrated circuit (IC) device was found to be on the order of 3 mm^3, this being the space surrounding the die. Therefore it was necessary to mininize dead space in the vacuum system to increase the chances of detecting any gasses present. The detector employed was a Quadrupole analyzer which possesses a variable range of 0 to 100 AMU. The sensitivity of the Faraday collector employed is 10^{-4} Amp/Torr for N_2 with a unit resolution and electrometer sensitivity of 10^{-6} Volts/Torr. A vacuum in the range of 10^{-6} to $4x10^{-6}$ Torr was achieved prior to the rupturing of the IC. Data collection consisted of photographs of the analyzer's CRT screen taken before, during, and after the event. Subsequent analysis of the photographs reveal the atomic mass of the gasses and ions of those gasses present inside the package.

CHAPTER 1

THEORETICAL BACKGROUND OF RESIDUAL GAS ANALYSIS

The setup of the Quadrupole 1210 residual gas analyzer consists of an ionizer filament and Faraday cage for intake, a system of three lenses to reduce interference at the detector, a quadrupole filter to remove any ions with an unsuitable m/e ratio, and a rigid Faraday collector tightly coupled to an electrometer to sense ion impact. An emission meter is used to monitor the filament current. The electrons boiled off by this current pass through a narrow aperture and cause a narrowly focused monoenergetic electron beam to enter the ionization chamber of the Faraday cage. The ionizing chamber is surrounded on four sides by the Faraday cage with an opening at either end. The Faraday cage operating at a voltage of +8V DC imparts this energy to the positive ions and moves them out of the Faraday cage toward the ion exit aperture, lenses, and filter rods. Ions exiting the ionizer must be within 30 degrees of the longitudinal axis of the filter in order to prevent collision with a filter rod or some other metal object before they reach the detector. Ions moving through the space surrounded by the filter rods are separated according to atomic mass. This mass filtering action is governed by the equations of motion of a charged particle traveling in the quadrupole analyzing field. A DC voltage, with superimposed RF voltage, is applied to the rods in a sawtooth form. Opposite pairs of rods are electrically connected, one pair having a

positive DC potential with zero degrees RF voltage, and the other pair with a negative DC potential and a 180 degree RF voltage. The RF and DC voltages are applied to the rods in the form of a sawtooth sweep. Both the RF and DC voltages increase from some low voltage to a higher value with their ratio remaining approximately constant. As the sweep progresses, ions pass through the filter in order of increasing atomic mass.

The potential at any point in the electric field within the rod array can be approximated by:

$$\Phi = (V_1 + V_0 \cos wt)(x^2 - y^2)/r^2 \qquad (1)$$

where; V_1 is the DC amplitude

V_0 is the RF amplitude

r is the field radius of the rectangular array, and

x and y are the perpendiculars to the axis of the quadrupole

Since $\nabla\Phi = E$, therefore:

$$E_x = -\partial\Phi/\partial x = -2(V_1 + V_0 \cos wt)\, x/r^2 \qquad (2)$$

$$E_y = -\partial\Phi/\partial x = -2(V_1 + V_0 \cos wt)\, y/r^2 \qquad (3)$$

$$E_z = -\partial\Phi/\partial x = 0 \qquad (4)$$

So the equations of motion for a singly charged ion of mass m injected

into this field in the z direction are:

$$my + (2e/r^2)(V_1 + V_0 \cos wt)\, y = 0 \qquad (5)$$

$$mx - (2e/r^2)(V_1 + V_0 \cos wt)\, x = 0 \qquad (6)$$

$$mz = 0 \qquad m\dot{z} = \text{constant} \qquad (7),(8)$$

From the equation $m\dot{z}$ = constant it is evident that the ion experiences no acceleration due to the quadrupole filter field. This indicates that the ion velocity is determined by the potential difference between the Faraday cage and the ground lens (ion energy). The velocity of any specific ion can be calculated from the relationship :

$$\dot{z} = (2eV_i/AM_H)^{.5} = 1.4*10^4 (V_i/A) \quad m/s \qquad (9)$$

where; V_i is the ion energy (volts)

M_h is the mass of the hydrogen atom (Kg)

A is the atomic weight of the particle (AMU)

e is the electron charge (coul)

By substitution of certain nondimensional quantities, equations (5) and (6) can be written as a linear second order differential equation with constant periodic coefficient which is also a normal form of the Mathieu equation. The characteristics of the solution of these equations determine the filtering action of the quadrupole.

$$x + \alpha(\beta + \cos\theta)\, x = 0 \qquad (10)$$

$$y - \alpha(\beta + \cos\theta)\, y = 0 \qquad (11)$$

where:

$\theta = wt$

$$\alpha = (e/m)\ 2V_0/r^2 w^2$$

$$\beta = V_1/V_0$$

ıese solutions of (10) and (11) possess regions where both x and y are .multaneously stable. The signifigance of this is that the resulting ion ·ajectory is stable and bounded, and the ion passes through the quadrupole .thout being captured by the rods. The largest of several regions of :ability is chosen for the operation of the mass spectrometer. The ırameters of α and β are used to define the region of stability (figure 1).

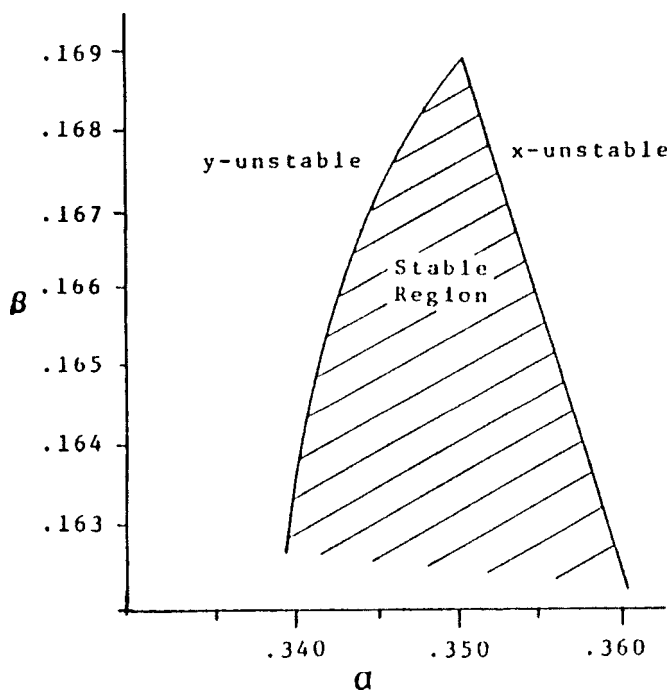

g. 1. The Stability Region for the QUAD 1210[1]

From the graph and the definition, of only ions with a certain range of charge-to-mass ratios will have stable trajectories for a given value of r, w and V_0. All ions with charge-to-mass ratios outside this range will collide with the quadrupole rods. As β approaches 0.168, the resolution of the instrument increases, but the total number of ions passed by the filter decreases. This provides a margin of compromise between resolution and sensitivity.

During normal operation, the QUAD1210 maintains a constant ratio of DC and RF voltages as well as a fixed value of both r and w. Filter selectivity is controlled by the RF voltage (V_0). Values for the QUAD1210 parameters are:

$r = 0.273$ cm	$e = 4.8*10^{-10}$ esu
$w = 1.57*10^{7}$ rad/sec	1 Volt = 1/300 erg/esu
$\alpha = 0.354$	1 AMU = $1.67*10^{-24}$ g

Thus for a singly charged ion the mass is;

$$m = \frac{(4.8*10^{-10}\ \text{esu})(1/300\ (\text{erg/esu})/\text{volt})(2V_0)}{(.354)(.273\ \text{cm})^2\ (1.57*10^{-7}\ \text{rad/sec})(1.67*10^{-24}\ \text{g/AMU})}$$

or

$$m = 0.294\ V_0\ \ \text{AMU/Volt}$$

CHAPTER 2

EXPERIMENTAL METHODS

A. PREPARATION OF THE IC

The package must first be connected to the alignment device by wrapping the pins of the package firmly around the device. Once this is accomplished, the package and alignment device must be affixed to the shaft of the lower bellows so that the epoxyed union of the package is fitted against the wedge attached to the lower bellows. This is followed by an acetone bath to eliminate the accumulation of oils due to handling. Then this assemblage is placed in the breaker vessel with an aluminum gasket between the conflat of the lower bellows and the throat of the vessel. An o-ring and washer combination is then placed around the shaft of the lower bellows that protrudes out of the vessel, and the top valve is seated and tightened down on the vessel to provide a vacuum seal (see figure 2). The entire system is then brought down to a pressure of approximately 8×10^{-5} Torr by a diffusion oil pump (figure 3). At this point the diffusion pump is disconnected and an ion pump is employed to reduce the pressure to 10^{-6} Torr (figures 4, 5). Bakeout is done to remove any gas clinging to the walls of the system or accelerate any out-gassing. After bakeout the detector is activated once the pressure is in the 10^{-5} Torr range so that the system can establish thermal equilibrium prior to rupturing the package.

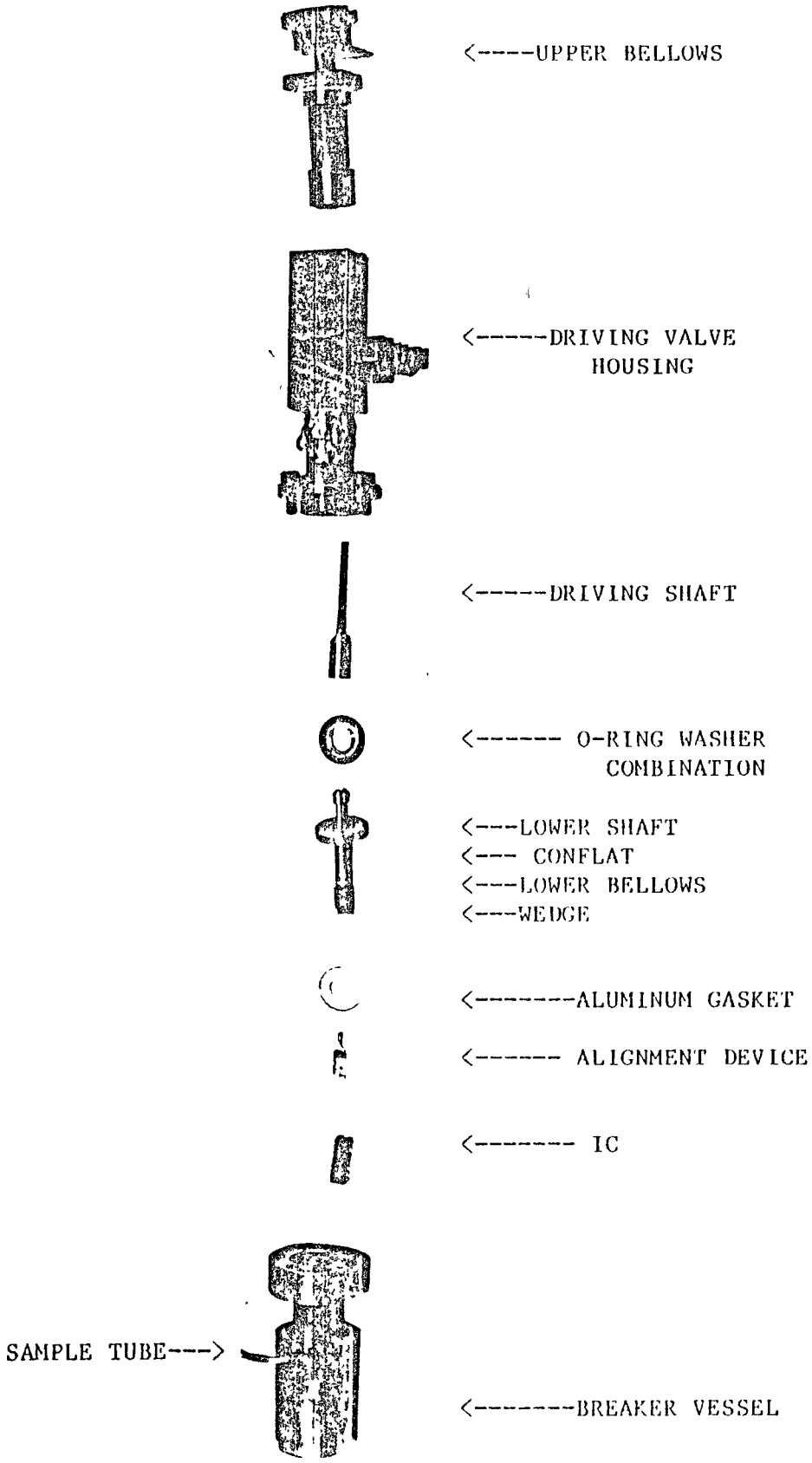

Fig. 2. Exploded view of the Packagebreaker

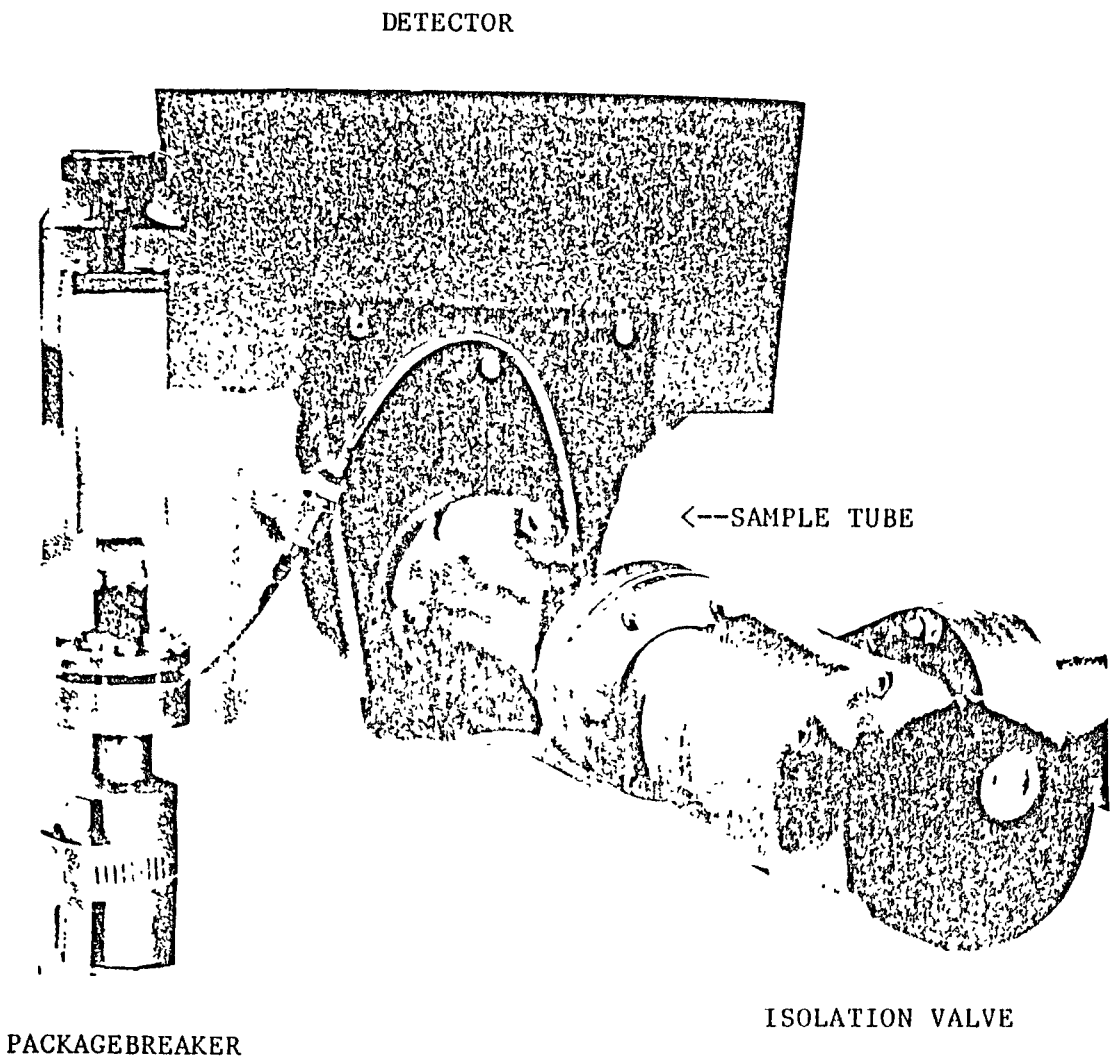

Fig. 4. Breaker-Detector System Segment

B. PROCEDURE

To rupture the IC package the upper valve is closed, driving the wedge between the ceramic slabs. No pressure rise is evident during or after rupture. At the time of rupture a motor driven camera is triggered recording approximately 12 sweeps through the AMU range of 0 to 60.

Data collected thus far is in the form of photographs of oscilliscope traces. By careful manual measurement of these photo traces the location of any peaks due to ion detection can be determined. A suitable conversion factor from the scale of the photographs to the actual AMU scale displayed on the oscilliscope was calculated. The measured photo trace is 64mm whereas the actual scope display was 100mm long representing a scale of 0 to 60 AMU. Thus the scope has a factor of .6 AMU/mm to the photo ratio of .9375 AMU/mm, indicating some loss of resolution. Another factor affecting the measurement of the ion peaks is the sweep rate. In order to produce a satisfactory picture the sweep rate was maximized, thus many peaks that would stand out at a lower rate are disguised in the trace as irregular peaks or a raised baseline level (see figure 8).

An alternate method employing the film negatives was also devised. The negatives were placed between two glass panes and projected on a grid using a slide projector and a flat focus lens. By varying the distance of the projector from the grid an optimal scale for measurement was determined. Data was then collected manually from the slides.

The settings for the equipment are as follows:

center mass 30

mass range 60

emission current .3 ma

resolution .66

verticle scale of oscilloscope .03 V/cm

pressure in system 10^{-6} Torr

The mass range and center mass controls are set for a horizontal scale of 0 to 60 AMU. Filament current emission is maintained at a low level to prolong filament life and protect against possible heavy oxygen content in the system. It was not possible to reduce pressure below the 10^{-6} level. This may be due to either a system leak or out-gassing of the device. Resolution was arrived at by trial and error and may require further optimization.

CHAPTER 3

INVESTIGATION OF THE DATA

A. ANALYSIS

Data was collected for four different devices. The device number and the method of data collection are listed as follows:

1. SN7404N S 7351	Visual inspection
2. *SW 741558 7233	Visual inspection
3. M MC7474L H2 7131	Motor driven camera
4. M MC5404L 7403	Motor driven camera

Analysis of the first two devices were done to verify that the chipbreaker design was actually workable and the results repeatable. The initial elation of the moment prevented detailed observation so the descriptions are somewhat lacking. Device 1 displayed relatively few lines on the lower end of the mass spectrum. Device 2 revealed a myriad of peaks across the entire range of the scale.

Device 3 was photographed by a motor driven camera, but in such a way that only a portion of the spectrum is visible in any one photograph (figure 6). Once this was dicovered the camera drive speed was reduced to permit full view of the atomic mass spectra. The data from device 3 can not be broken into time frames due to the fragmentation of the spectrum.

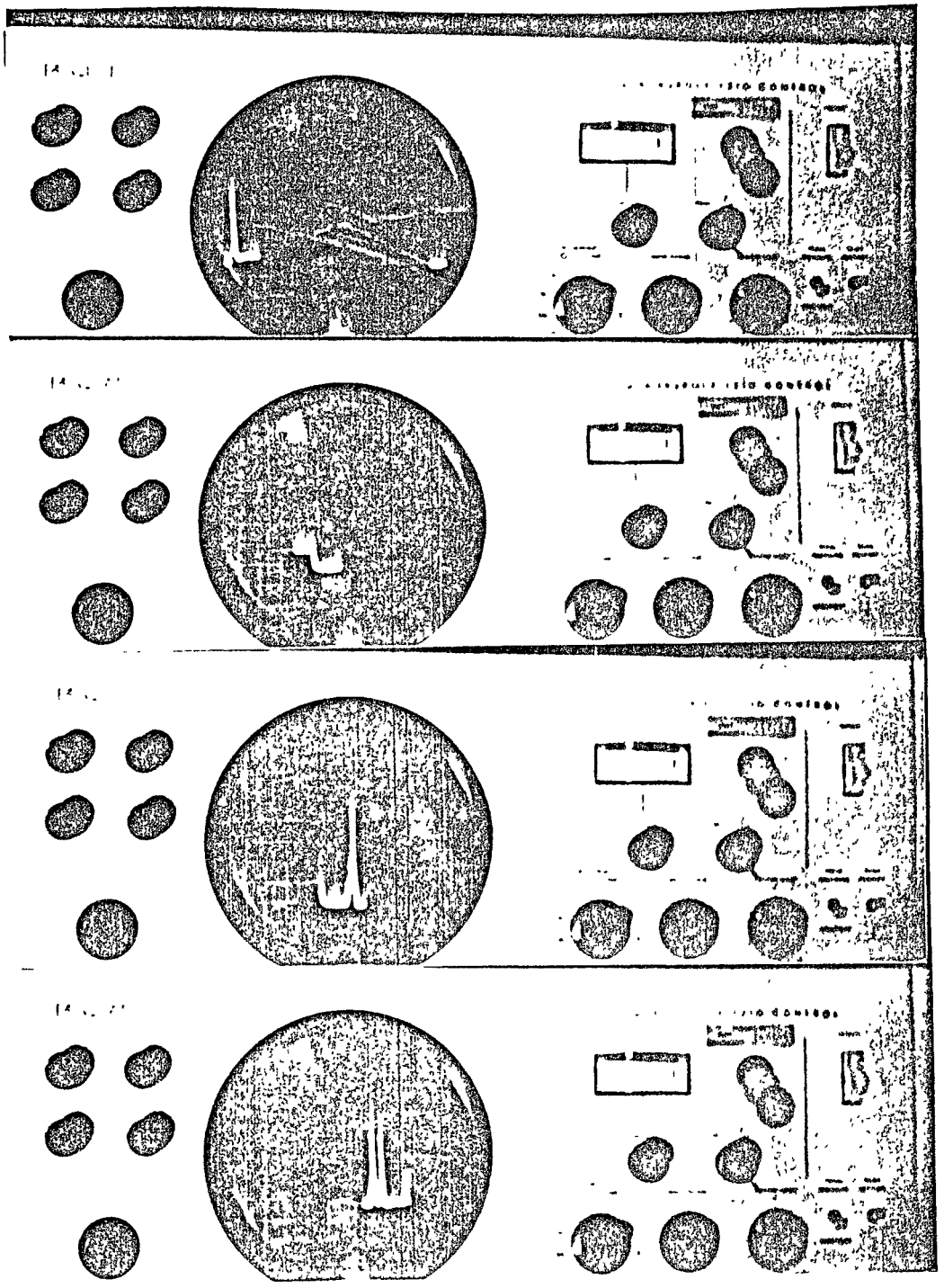

Fig. 6. Segmented Data Samples from Device 3

The results of the measurement of all photos taken are shown in table 1.

TABLE 1

RESIDUAL GASES PRESENT IN DEVICE 3

AMU	MOST PROBABLE ION PARENT	SECOND MOST PROBABLE ION PARENT
2	H_2	He
18	H_2O	NH_3
30	C_2H_6	C_3H_8
32	O_2	SO_2
37	Cl	C_3H_8
40	Ar	
42	C_3H_8	CH_3COCH_3
44	CO_2	
48	SO_2	
54	CH_3COCH_3	

Device 4 provided the best data obtained thus far. The motor drive speed caused an overlap of the traces in some instances and the time intervals between the photos are only approximate. Despite the existing problems the data obtained is in a usable form. The data photographs are shown in figures 7 through 20. Data obtained from measuring these photographs are contained in tables 2 through 14. The reference table for probable ion parents is shown in table 15.

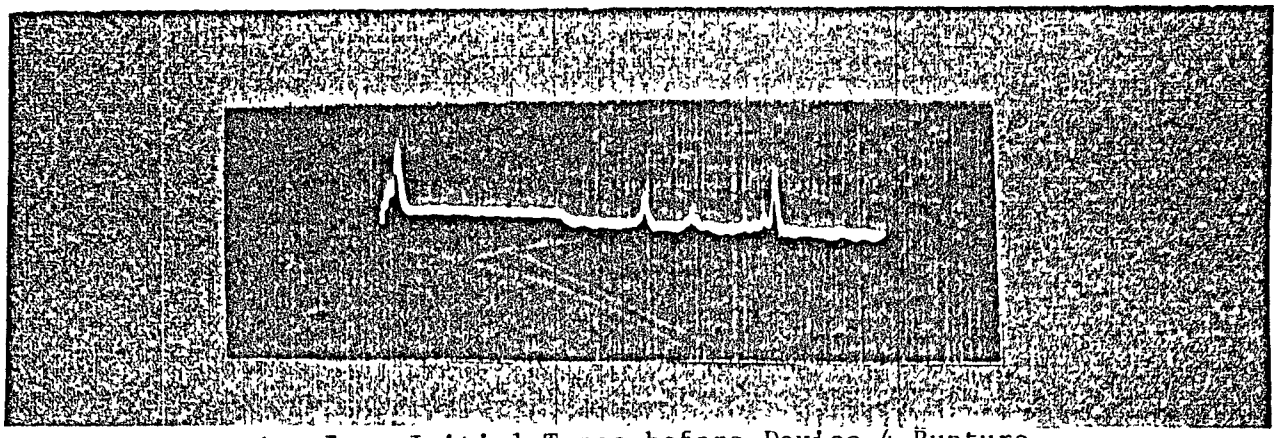

Fig. 7. Initial Trace before Device 4 Rupture

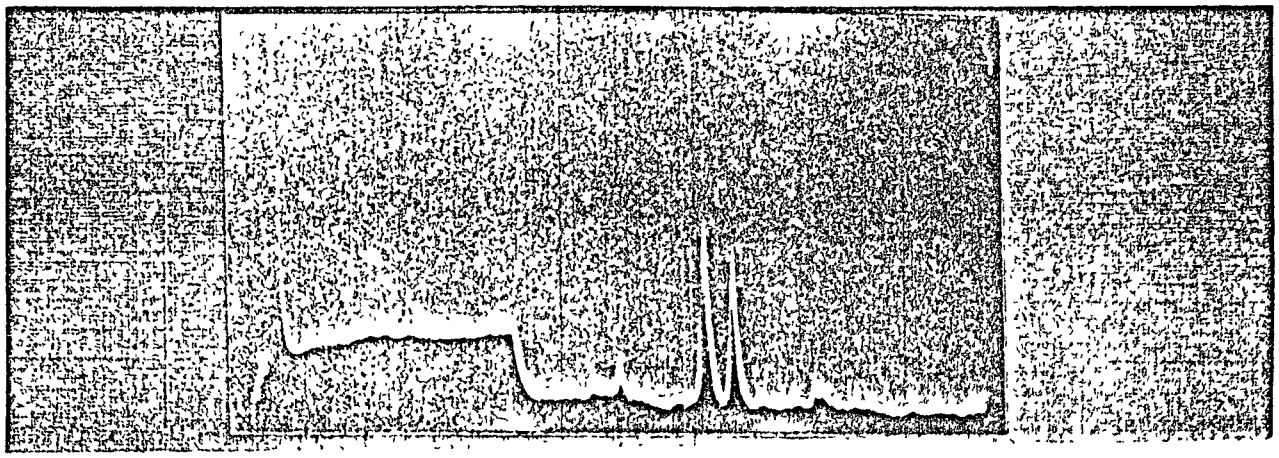

Fig. 8. Immediatly after Device 4 Rupture

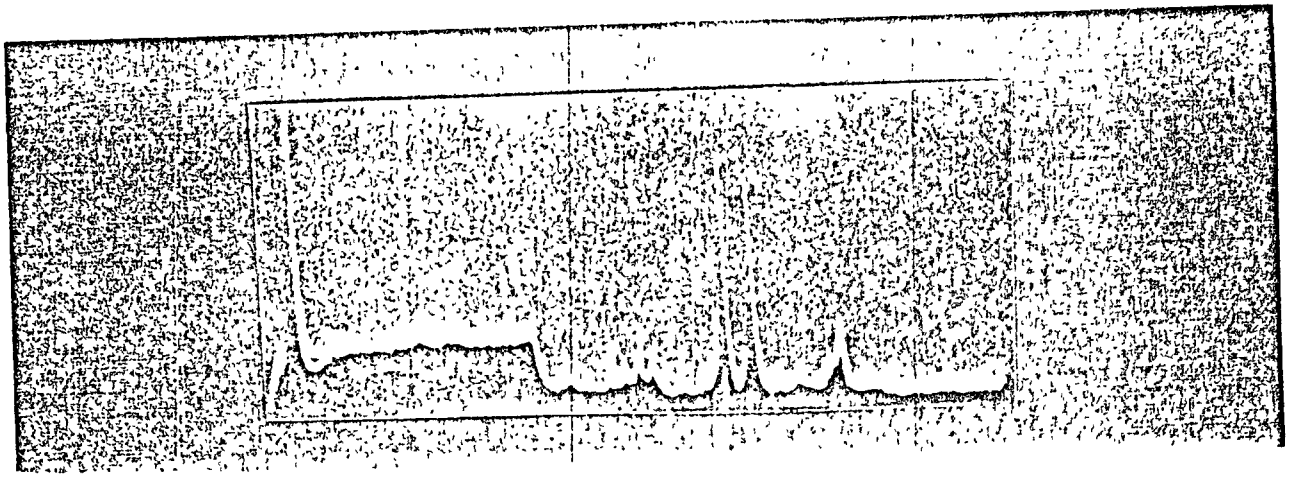

Fig. 9. .41 Seconds after Device 4 Rupture

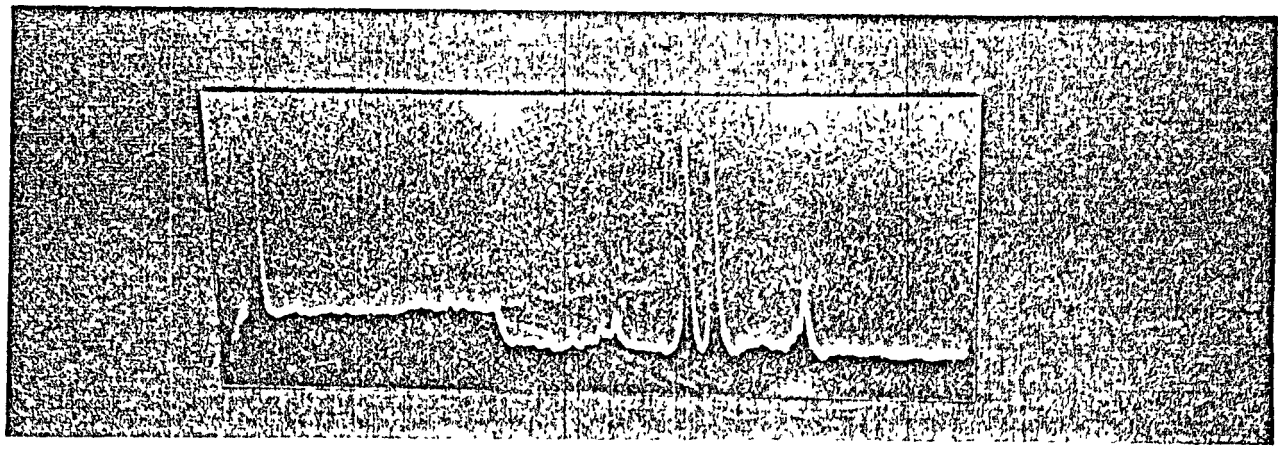

Fig. 10. .82 Seconds after Device 4 Rupture

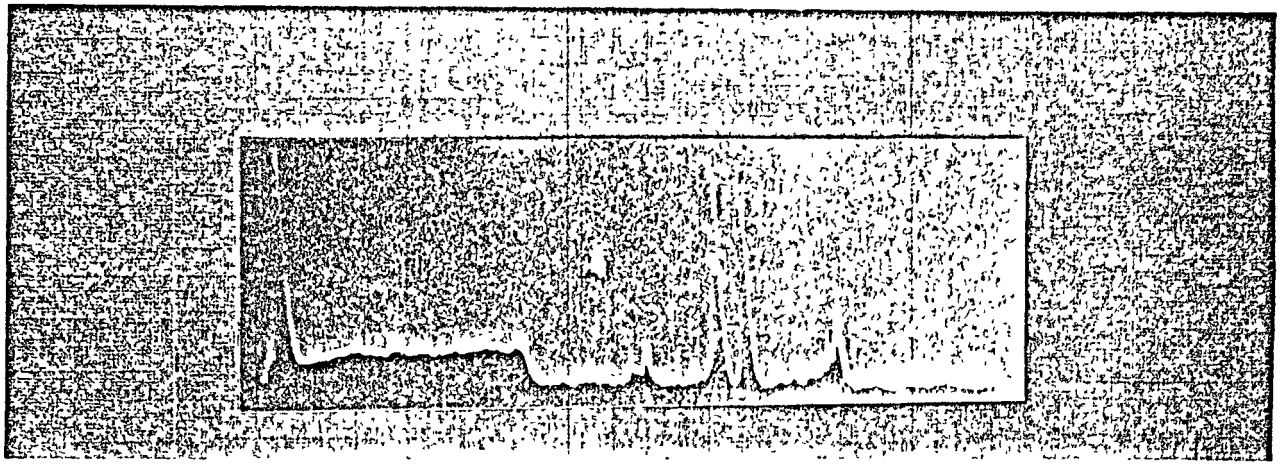

Fig. 11. 1.23 Seconds after Device 4 Rupture

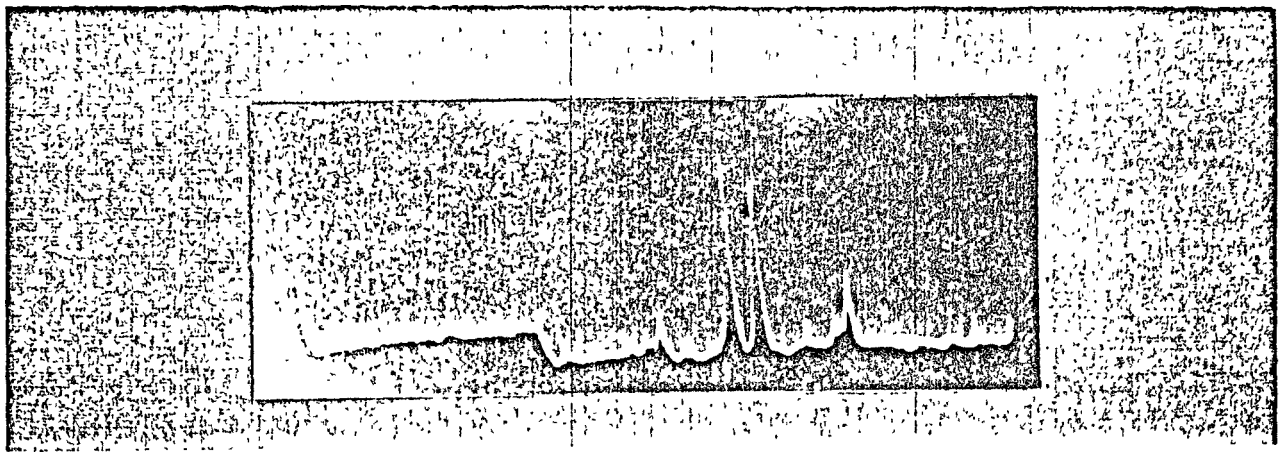

Fig. 12. 1.64 Seconds after Device 4 Rupture

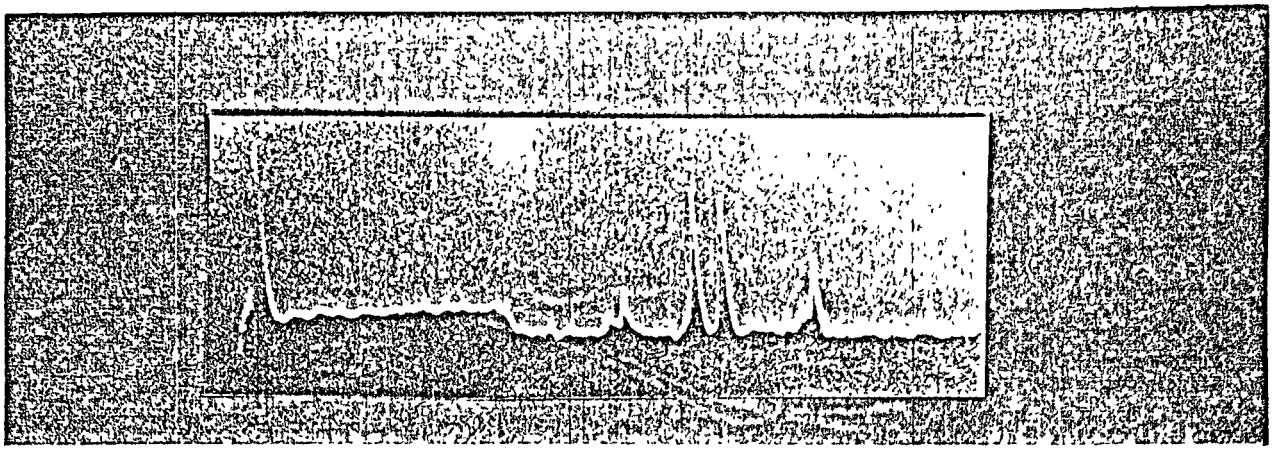

Fig. 13. 2.05 Seconds after Device 4 Rupture

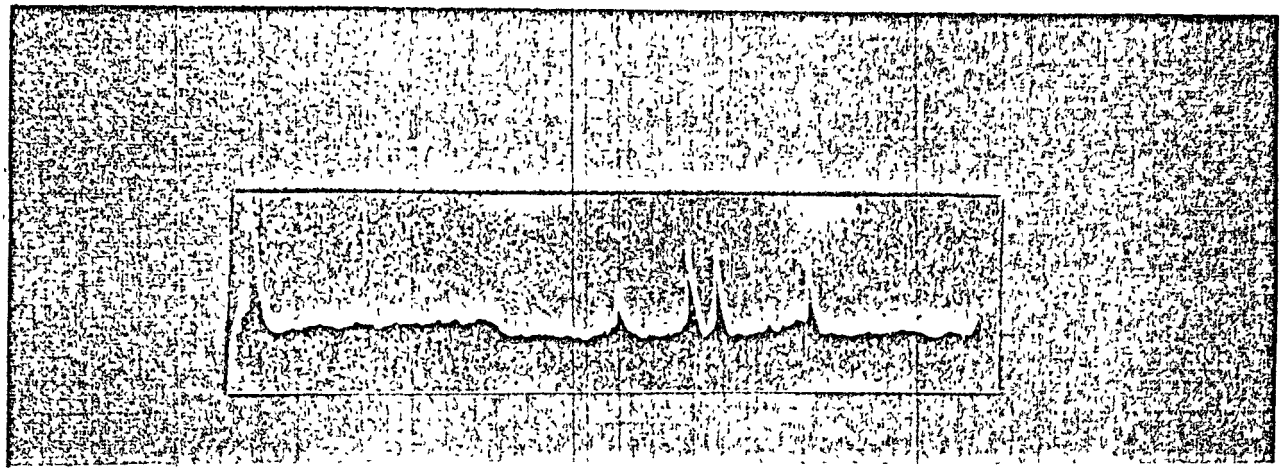

Fig. 14. 2.46 Seconds after Device 4 Rupture

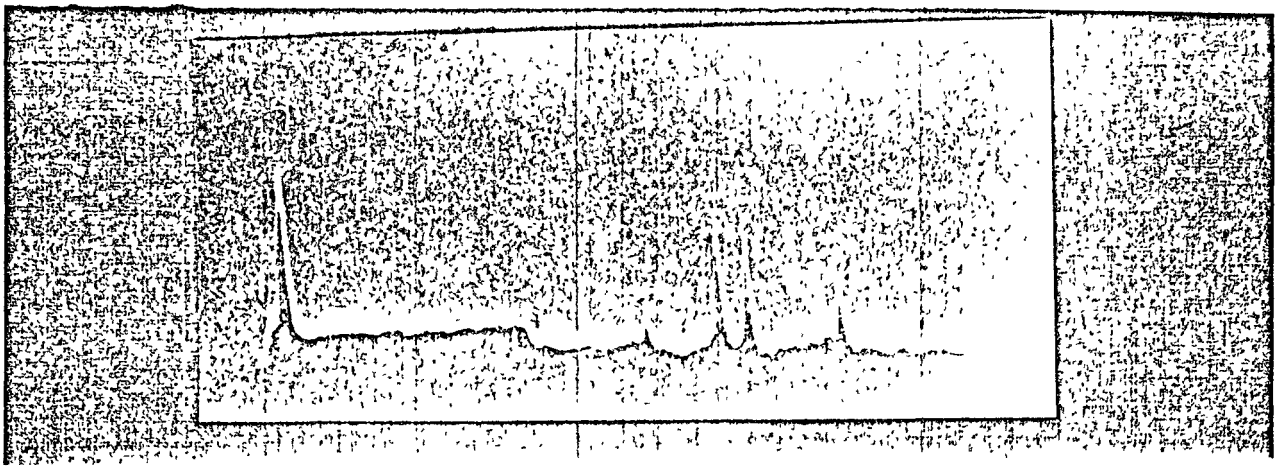

Fig. 15. 2.87 Seconds after Device 4 Rupture

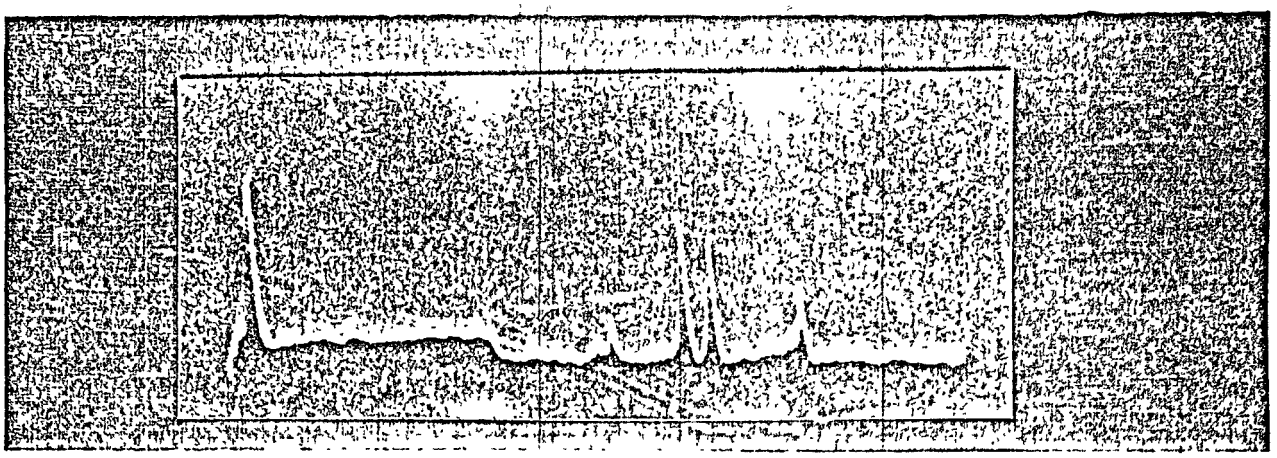

Fig. 16. 3.28 Seconds after Device 4 Rupture

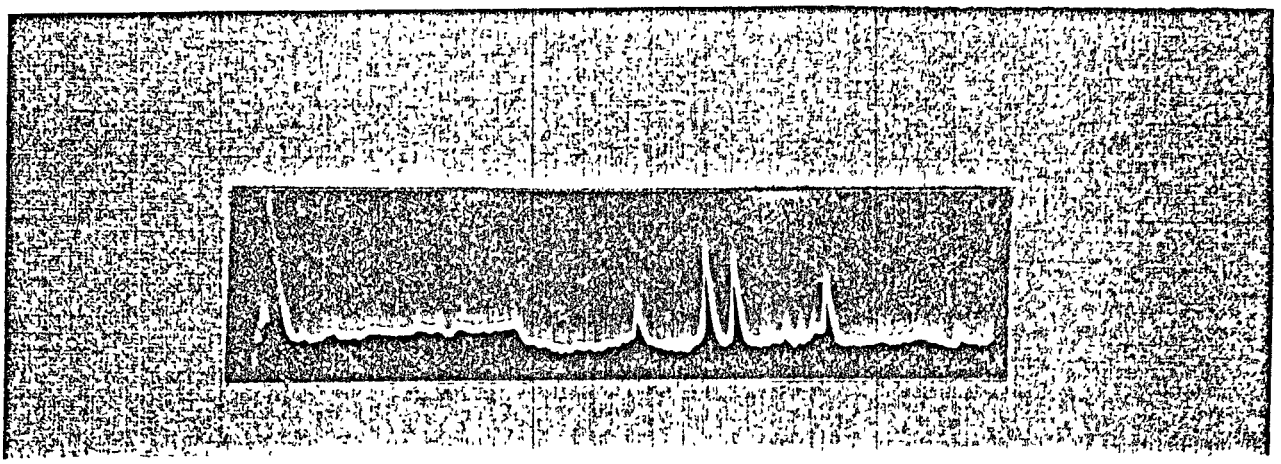

Fig. 17. 3.69 Seconds after Device 4 Rupture

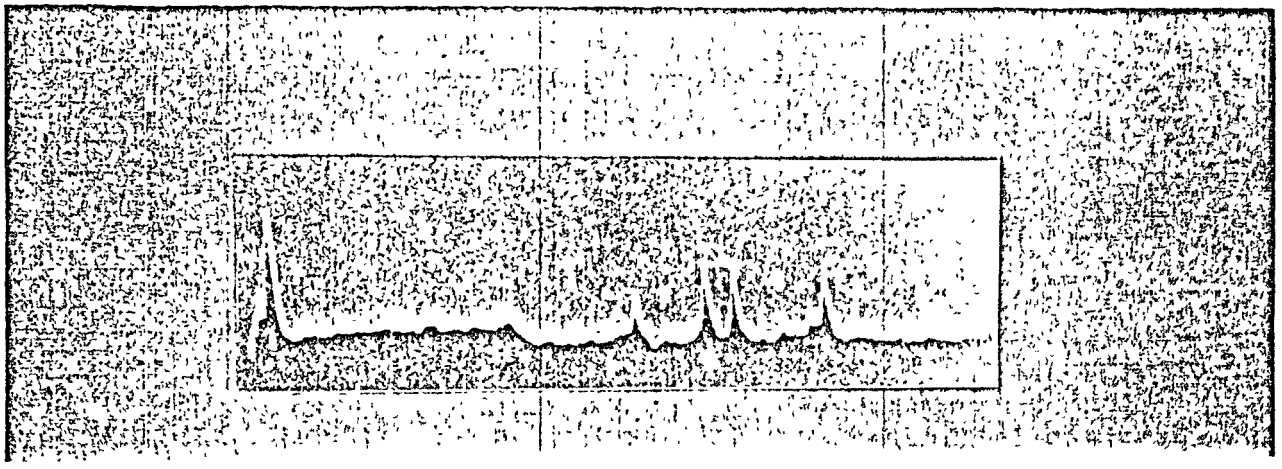

Fig. 18. 4.10 Seconds after Device 4 Rupture

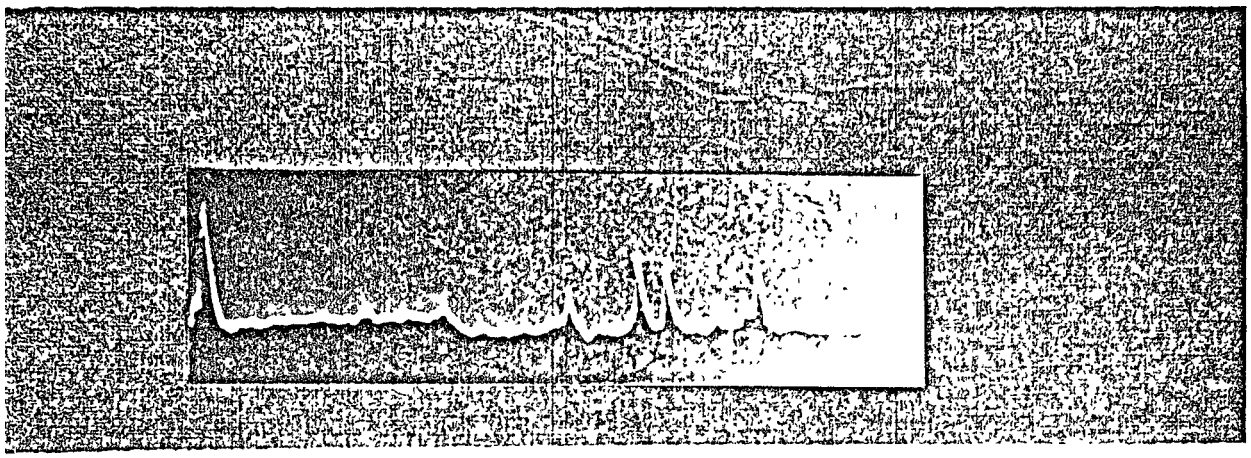

Fig. 19. 4.51 Seconds after Device 4 Rupture

TABLE 2

DATA OBTIANED FROM THE ANALYSIS OF FIGURE 7

AMU	MOST PROBABLE ION PARENT	SECOND MOST PROBABLE ION PARENT	POSSIBLE ETCHANT IONS		
2	H_2	He	H		
32	O_2	SO_2	O	CH_3CO	S
37	Cl	C_3H_8	HCl	F_2	
48	SO_2		PO	SO	CCl

TABLE 3

DATA OBTAINED FROM THE ANALYSIS OF FIGURE 8

AMU	MOST PROBABLE ION PARENT	SECOND MOST PROBABLE ION PARENT	POSSIBLE ETCHANT IONS		
1	H_2O	CH_4	H		
2	H_2	He	H_2		
20	F		Ne	BeH	
21	Ne	Ar			
25	C_2H_6	C_3H_8	BeO	BN	
27	N_2	CO_2			
32	O_2	SO_2	O_2	CH_3CO	S
35	Cl		Cl		
37	Cl	C_3H_8	HCl	F_2	
44	CO_2	C_3H_8			
48	SO_2		PO	SO	CCl
57	CH_3COCH		CCl	F_3	

TABLE 4

DATA OBTAINED FROM THE ANALYSIS OF FIGURE 9

AMU	MOST PROBABLE ION PARENT	SECOND MOST PROBABLE ION PARENT	POSSIBLE ETCHANT IONS		
2	H_2	He	H_2		
12	CH_4	CO	C	BH	
24	C_2H_6	C_3H_8	C_2		
30	C_2H_6	C_3H_8		NO	
31	CH_3COCH_3	C_2H_6	P	CF	HNO
37	Cl	C_3H_8	HCl	F_2	
40	Ar		Ne_2	H_2F_2	Ar
43	CH_3COCH_3	C_3H_8	N_2O	CO_2	
51	SO_2		CF		

TABLE 5

DATA OBTAINED FROM TNE ANALYSIS OF FIGURE 10

AMU	MOST PROBABLE ION PARENT	SECOND MOST PROBABLE ION PARENT	POSSIBLE ETCHANT IONS		
2	H_2	He	H_2		
4	He	CH	He		
*					
*	H_2O	NH_3	OH	NH_3	NH_4
*					
21	Ne		Ne	BeH	
22	F		B_2		
30	C_2H_6	C_3H_8		NO	
32	O_2	SO_2	O_2	CH_3CO	S
37	Cl	C_3H_8	HCl	F_2	
40	Ar		Ne_2	H_2F_2	Ar
48	SO_2				

*NOTE: Due to the trace in figure 10 from the range of 4 to 20 AMU was the most defined, some possible ions that could be found in that range are listed in this table. Clear distinctions of peaks were not possible so only a general class of ions are included.

TABLE 6

DATA OBTAINED FROM THE ANALYSIS OF FIGURE 11

AMU	MOST PROBABLE ION PARENT	SECOND MOST PROBABLE ION PARENT	POSSIBLE ETCHANT IONS		
2	H_2	He	H_2		
20	Ne	Ar			
30	C_2H_6	C_3H_8		NO	
32	O_2	SO_2	O_2	CH_3CO	S
37	Cl	C_3H_8	HCl	F	
40	Ar		Ne_2	H_2F_2	Ar
44	CO_2				
48	SO_2				
55	CH_3COCH_3	CH_3COCH_3			

TABLE 7

DATA OBTAINED FROM THE ANALYSIS OF FIGURE 12

AMU	MOST PROBABLE ION PARENT	SECOND MOST PROBABLE ION PARENT	POSSIBLE ETCHANT IONS		
2	H_2	He	H_2		
14	CH_4	N_2	N	CH_2	
22	Ne		B_2		
30	C_2H_6	C_3H_8		NO	
31	CH_3COCH_3	C_2H_6	P	CF	HNO
37	Cl	C_3H_8	HCl	F_2	
40	Ar		Ne_2	H_2F_2	Ar
42	C_3H_8	CH_3COCH_3			
45	CH_3COCH_3	CH_3COCH_3	CO_2		
55	CH_3COCH_3	CH_3COCH_3			
57	CH_3COCH_3	CH_3COCH_3	CCl	F_3	

TABLE 8

DATDA OBTAINED FROM THE ANALYSIS OF FIGURE 13

AMU	MOST PROBABLE ION PARENT	SECOND MOST PROBABLE ION PARENT	POSSIBLE ETCHANT IONS		
2	H_2	He	H_2		
24	C_2H_6	C_3H_8	C		
26	C_2H_6	C_3H_8	CN		
37	Cl	C_3H_8	HCl	F	
40	Ar		Ne_2	H_2F_2	Ar
56	CH_3COCH_3		CCl		

TABLE 9

DATA OBTAINED FROM THE ANALYSIS OF FIGURE 14

AMU	MOST PROBABLE ION PARENT	SECOND MOST PROBABLE ION PARENT	POSSIBLE ETCHANT IONS		
2	H_2	He	H_2		
12	CH_4	CO	C	BH	
28	N_2	CO_2	BeF	CO	C_2H_4
31	CH_3COCH_3	C_2H_6	P	CF	HNO
37	Cl	C_3H_8	HCl	F_2	
40	Ar		Ne_2	H_2F_2	Ar
48	SO_2		PO	SO	CCl
58	CH_3COCH_3		BO_3	CNO_2	

TABLE 10

DATA OBTAINED FROM THE ANALYSIS OF FIGURE 15

AMU	MOST PROBABLE ION PARENT	SECOND MOST PROBABLE ION PARENT	POSSIBLE ETCHANT IONS		
2	H_2	He	H_2		
31	CH_3COCH_3	C_2H_6	P	CF	HNO
37	Cl	C_3H_8	HCl	F_2	
40	Ar		Ne_2	H_2F_2	Ar
45	CH_3COCH_3		CO_2		
50	SO_2				

TABLE 11

DATA OBTAINED FROM THE ANANLYSIS OF FIGURE 16

AMU	MOST PROBABLE ION PARENT	SECOND MOST PROBABLE ION PARENT	POSSIBLE ETCHANT IONS		
1	H_2O	CH_4	H		
2	H_2	He	H_2		
26	C_2H_6	C_3H_8	CN	AL	
32	O_2	SO_2	O_2	CH_3CO	S
37	Cl	C_3H_8	HCl	F	
40	Ar		Ne_2	H_2F_2	Ar
55	CH_3COCH_3				

TABLE 12

DATA OBTAINED FROM THE ANALYSIS OF FIGURE 17

AMU	MOST PROBABLE ION PARENT	SECOND MOST PROBABLE ION PARENT	POSSIBLE ETCHANT IONS		
2	H_2	He	H_2		
13	CH_4		CH	BH	
15	CH_4	CH_3COCH_3	O	CH_3	NH
17	NH_3	H_2O	OH	NH_3	
32	O_2	SO_2	O_2	CH_3CO	S
37	Cl	C_3H_8	HCl	F_2	
40	Ar		Ne $_2$	H_2F_2	Ar
43	C_3H_8	CH_3COCH_3	C_3H_8	N_2O	CO_2
44	CO_2	C_3H_8			
45	CH_3COCH_3		CO_2		
57	CH_3COCH_3		CCl	F_3	

TABLE 13

DATA OBTAINED FROM THE ANALYSIS OF FIGURE 18

AMU	MOST PROBABLE ION PARENT	SECOND MOST PROBABLE ION PARENT	POSSIBLE ETCHANT IONS		
2	H_2	He	H_2		
32	O_2	SO_2	O_2	CH_3CO	S
37	Cl	C_3H_8	HCl	F_2	
40	Ar		Ne	H_2F_2	Ar
43	C_3H_8	CH_3COCH_3	C_3H_8	N_2O	CO_2
48	SO_2		PO	SO	CCl
51	SO_2		CF_2		
57	CH_3COCH_3		CCl	F_3	

TABLE 14

DATA OBTAINED FROM THE ANALYSIS OF FIGURE 19

AMU	MOST PROBABLE ION PARENT	SECOND MOST PROBABLE ION PARENT	POSSIBLE ETCHANT IONS		
1	H_2	H_2O	H		
2	H_2	He	H_2		
15	CH_4	NH_3	O	CH_3	NH
20	Ne	Ar			
22	Ne		B		
37	Cl	C_3H_8	HCl	F_2	
39	Cl	C_3H_8			
40	Ar	C_3H_8	Ne	H_2F_2	Ar
43	CO_2	C_3H_8	C_3H_8	N_2O	CO_2
48	SO_2		PO	SO	CCl

TABLE 15

TYPICAL MASS PATTERNS FOR RESIDUAL GAS ANALYZERS

Parent →	H_2	He	CH_4	NH_3	H_2O	F	Ne	F_2	CO	C_2H_6	O_2	Cl	Ar	CO_2	C_3H_8	SO_2	CH_3COCH_3
1	0.8%		1%	0.3%	6%					0.4%					0.8%		0.5%
2	100%	2.4%	2.4%		2.2%					1%					2.7%		
3																	
4		100%															
5																	
6																	
7																	
8																	
9																	
10																	
11																	
12			2.1%						2%	0.3%				1.7%	0.4%		1.1%
13			4.8%							0.5%					0.6%		2.6%
14			11%	2.5%				5.5%	0.8%	1.3%					2.7%		8.6%
15			80%	7.3%						7.3%					4.6%		44%
16			100%	93%	2.3%				1%	0.3%	7.1%			4.8%	0.5%	3.6%	0.1%
17				100%	25%												
18				2.3%	100%												
19						100											2.5%
20							100%						20%				
21							0.3										
22							9.9%										
23																	
24										0.3%					0.3%	1.5%	0.3%
25										3%					1.3%		1.5%
26										19%					10%		5.5%
27										30%					44%		7.7%
28								100%	100%	100%				13%	96%		1.9%
29									1%	21%					100%		4.4%
30									0.3%	56%					6.7%		0.2%
31										0.6%							0.7%
32											100%					8.6%	
33																0.1%	
34																0.4%	
35												100%					
36															1%		0.6%
37												30%			4.8%		2.1%
38															7.4%		2.3%
39															71%		3.5%
40													100%		5%		1.2%
41															18%		2.0%
42															7%		8.9%
43															36%		100%
44														100%	42%		2.5%
45																	0.2%
46																	
47																	
48																1.1%	
49																0.5%	
50																2.4%	
51																	
52																	0.1%
53																	0.4%
54																	
55																	0.1%
56																	
57																	0.8%
58																	79%
59																	0.9%
60																	0.1%
61																	
62																	
63																	
64																100%	
65																0.9%	
66																1.8%	

SOURCE: Instruction manual for Partial Pressure Gauge no. 974-0035 and Control Unit Model no. 974-0036. Palo Alto, Ca. Varian Vacuum Division, 1969. p. 18.

B. ION ANALYSIS

The main problem with using the table of probable ions supplied with the residual gas analyzer is that the circumstances are unique. The gases that may normally occur in such a system are not always associated with semiconductor devices. Because of this, a table of chemicals and gases used in alumina etching was compiled to find alternate possibilities for various AMU values. Tables 16 and 17 show lists of materials used in IC fabrication. Tables 18 and 19 show the materials used in Al etching in TTL and MOS circuits. Following these is a table of elements involved with the etching process with their corresponding AMU values. When viewed in this way, it is evident that some of these elements could be responsible for some of the peaks in the data. If this is the case then the probability of active etchant chemicals existing inside the device is very great. Tables 2 through 14 show the standard residual gases along with possible ions generated from etchant chemicals. Additional combinations of elements may be devised by observing the elemental AMU values at the bottom of table 19 and matching viable combinations with existing peaks in the data.

Other fabrication processes may be the governing factor in the gas content of the device. Masking chemicals or gases, doping chemicals, etc. are listed in tables 16 and 17. Another possiblity is the environment in which the device is sealed, which is unknown to the author at this time.

TABLE 16

SOLID MATERIALS DEPOSITED AND REMOVED WITH GASES USED FOR THE PLASMA PROCESS.

SOLIDS	GASES
DEPOSITIONS	
Silicon nitride	Silane (SiH_4), ammonia (NH_3)
Silicon oxide	Nitrous oxide (N_2O), SIH_4
Amorphous silicon	SiH_4 and argon
MATERIAL REMOVAL	
Silicon oxide	Silicon tetrafloride (SiF_4) Carbon tetrafloride (CF_4) C_3F_8, C_2F_6, C_5F_{12}, CHF_3, CF_4 and O_2
Silicon	CF_4 and O_2 Carbon tetrachloride (CCl_4) and hydrogen chloride (HCl)
Silicon nitride (Si_3N_4)	CF_4
Vanadium, titanium	CF_4
Tantalum, tungsten	CF_4
Molybdenum	CF_4
Chrome and chrome oxide	CCl_4
Aluminum	CCl_4, Boron trichloride (BCl_3)
Photoresist	Argon and O_2

TABLE 17

CHEMICALS USED IN ASSEMBLY
Trichloroethylene
Vapor degreasers
Ultrasonic degreasers
Nitrogen
Other reducing atmospheres
Flux
Solder paste

CHEMICALS USED IN CAPACITOR CONSTRUCTION
Silicon oxide
Aluminum oxide
Tantalum oxide
Tantulum pentoxide

CHEMICALS USED IN FILM RESISTOR CONSTRUCTION
Alumina
Beryllia
Copper
Kovar
Lead borosilicate

TABLE 18

CHEMICALS USED FOR ETCH PREPARATION
HF
HNO_3

DOPING CHEMICALS	
SOLUTIONS	GASES
$SiCl_4$	B_2H_6
PCl_5	AsH_3
$SbCl_5$	PH_3

ETCHANT FORMULAS FOR ALUMINA SUBSTRATES		
Aluminum,pure	phosphoric acid	80%
	nitric acid	5%
	acetic acid	5%
	water	10%
Aluminum,alloys	dilute ferric chloride	
	hydrochloric acid	20-50% by volume
	some nitric added to protect Ti parts	
Anodized aluminum	chromic acid	(no)
	phosphoric acid	(attack on)
	water	(aluminum)

TABLE 19

REACTIVE ION ETCHANTS OF ALUMINUM ALLOYS USED IN MOS CIRCUITS.

$SiCl_4$
CCl_4
BCl_3
CCl_2F_2
PCl_3
HCl

Cl_2

SOME WEIGHTS OF POSSIBLE ETCHANT IONS FORMED DURING IONIZATION

ELEMENT	AMU
H	1
B	11
C	12
N	14
O	16
F	19
Ne	20
Al	27
P	31
S	32
Cl	35-36
Ar	40

C. CONCLUSIONS

The system design was proved capable of measuring the small volume of gases present in ceramic dip packages. Device 3 was identified as a TTL D type flip flop manufactured in week 31 of 1971 by Motorola. Device 4 was identified as a TTL hex inverter manufactured in week 3 of 1974 by Motorola. Initial findings indicated that there are many substances inside the ceramic package devices that are detectable by the instrumentation used.

Analysis of the gases contained in devices 3 and 4 were performed under the assumption of typical residual gas analyzer readings and by examining possible ions involved in the fabrication process. In order to positively identify the gases present in a device, calibration sources must be used in combination with a better data acquisition method. Additional research should be done to determine the feasability of residual gas analysis of ceramic dip pack devices and to5, to18 metal packaged devices. Some suggesstions for further research have been put forth in chapter 4.

CHAPTER 4

SUGGESTIONS FOR FUTURE RESEARCH

A. PACKAGEBREAKER ADDITIONS AND MODIFICATIONS

A starting point would be the removal of all o-rings from the system. These points should be replaced by heliarc or a conflat and metal gaskets. To reduce turnaround time for investigations, a high quality vacuum valve should be installed between the breaker and the detection system. This would prevent unwanted oxidation of the detector filaments and reduce the amount of both bake-out and pump time. If possible the breaker should be adapted for the t05 and t018 metal packages. This might be accomplished through the use of a hardened steel needle attachment for the present design. The needle should be hollow and have vent holes at strategic locations. An important addition to the packagebreaker would be a power feedthrough. Such a device would permit the observation of powered up outgassing by semiconductor layers and any gettering by the conductant strips.

B. SYSTEM ADDITIONS AND MODIFICATIONS

To reduce the inherent outgassing in the system, all O-ring valves should be replaced. A calibration system for various gases and fabrication chemicals should be fashioned. The purpose of such a calibration device is to aid in the identification of corrosives present in the devices being tested. A high speed analog to digital converter

connected to the detector output and interfaced with a microprocessor could be used in conjunction with the calibration system to form a database of different etchants and chemicals. In addition the A/D microprocessor interface would facilitate background subtraction and provide a more accurate method of measuring peak locations.

C. PREPARATION OF THE CERAMIC PACKAGE

Initially the ceramic device should be scrubbed in a flow of Freon 115 with a light brush. This should be followed by an ultrasonic rinse in deionized water. The package holder and breaker parts must be treated in a similar manner to insure the removal of all oils and salts. From this point all handling must be done with gloves and clean instruments. The package should be connected to a combination alignment-power feedthrough device and placed in the breaker vessel. Once this is done the bellows and wedge assembly should be placed over a metal gasket in the throat of the vessel and the system sealed by bolting the driving mechanism onto the vessel. The detector system should already be pumped down to the 10^{-5} Torr range. Proceed with a brief bakeout of the vessel and system. Allow a period of time after bakeout for the system to achieve thermal equlibrium.

D. DATA ACQUISITION

Background readings should be taken by the A/D micro processor interfaced with the Quadrupole RF sweep. The readings should be placed in secondary storage. After closing the sample tube valve, the package should

be ruptured and preparations made for data acquisition by the microprocessor system. Open the sample valve and record the data for a set period. Close the sample valve. Place all readings in secondary storage. Power should be put to the device and time given to establish thermal equlibrium. Open the sample valve and record data for a set period of time. Place the data in secondary storage.

Repeat the procedure with a device from the same lot but with the power on during acquisition of the first data set and the power off during the second data set. Repeat the entire process then with a device from the same lot under continuous bakeout.

Ideally the all of the techniques of data collection should be repeated a number of times in order to form a statistical database. This may not always be possible.

REFERENCES

1. Instruction manual for the Residual Gas Analyzer Model 1210.(Palo Alto, Ca.:Electronic Associates Inc., 1971), p. A-4.

2. Reference 1, p. A-4.

BIBLIOGRAPHY

Instruction manual for the Residual Gas Analyzer Model 1210. Palo Alto, Ca.:Electronic Associates Inc., 1971.

Anderson, R. E.. Operation of diffusion pumps. Personal communication. Spring 1986.

Silvus, H. S.. IC cleaning and preparation Personal communication. Spring 1986.

Crawford, J. R.. The measurement of photographic data. Personal communication. Spring 1986.

Jones, Roydn J.. Hybrid Circuit Design and Manufacture. New York, Marcel Dekker inc., 1982.

Instruction Manual for Partial Pressure Gauge no. 974-0035 and Control Unit Model no. 974-0036. Palo Alto, Ca. Varian Vacuum Division, 1969.

Fogiel, M. and others. Modern Microelectronic Circuit Design, IC Applications, Fabrication Technology Vol.1,Vol.2. New York. Research and Education Association, 1982.

LeBeau, Barry, and Wourms, Bob. Characterization of Al-Si Plasma Etching and it's Affect on Metal Oxide Semiconductor (MOS) Parameters. The Society of Photo-Optical Instrumentation Engineers. San Jose, Ca., 1980.

Elliot, David J. Integrated Circuit Fabrication Technology. Mcgraw-Hill Inc., New York, 1982.

Meeker, George E.. Welding and Metallurgy. Personal communication, Spring 1986.